

# Magnetic detection of high mechanical stress in iron-based materials using eddy currents and phase shift measurements

Cite as: J. Appl. Phys. **129**, 243901 (2021); <https://doi.org/10.1063/5.0050402>

Submitted: 15 March 2021 . Accepted: 03 June 2021 . Published Online: 22 June 2021

M. S. García Alonso,  A. Hernando,  J. Vinolas, and  M. A. García



View Online



Export Citation



CrossMark

## ARTICLES YOU MAY BE INTERESTED IN

[Recent developments of quantum sensing under pressurized environment using the nitrogen vacancy \(NV\) center in diamond](#)

Journal of Applied Physics **129**, 241101 (2021); <https://doi.org/10.1063/5.0052233>

[Characteristics of continuous high power magnetron sputtering \(C-HPMS\) in reactive O<sub>2</sub>/Ar atmospheres](#)

Journal of Applied Physics **129**, 243301 (2021); <https://doi.org/10.1063/5.0051296>

[Compact explicit matrix representations of the flexoelectric tensor and a graphic method for identifying all of its rotation and reflection symmetries](#)

Journal of Applied Physics **129**, 244103 (2021); <https://doi.org/10.1063/5.0048386>



Webinar  
How to Characterize Magnetic  
Materials Using Lock-in Amplifiers

Zurich  
Instruments

CRYOGENIC

Register now

# Magnetic detection of high mechanical stress in iron-based materials using eddy currents and phase shift measurements

Cite as: J. Appl. Phys. 129, 243901 (2021); doi: 10.1063/5.0050402

Submitted: 15 March 2021 · Accepted: 3 June 2021 ·

Published Online: 22 June 2021



View Online



Export Citation



CrossMark

M. S. García Alonso,<sup>1,2,3</sup> A. Hernando,<sup>2,3,4,5</sup>  J. Vinolas,<sup>2</sup>  and M. A. García<sup>1,a)</sup> 

## AFFILIATIONS

<sup>1</sup>Instituto de Cerámica y Vidrio (ICV), CSIC, Kelsen 5, 28049, Madrid 28240 Spain

<sup>2</sup>Universidad Antonio de Nebrija, Calle de los Pirineos, 55, Madrid 28040 Spain

<sup>3</sup>Instituto de Magnetismo Aplicado, Salvador Velayos, UCM-CSIC-ADIF, Las Rozas, Madrid E-28230, Spain

<sup>4</sup>IMDEA Nanociencia, C/Faraday 9, 28049 Madrid, Spain

<sup>5</sup>Donostia International Physics Center, Universidad del País Vasco, C/Manuel de Lardizabal 5, 20018 San Sebastian, Spain

<sup>a)</sup>Author to whom correspondence should be addressed: [magarcia@icv.csic.es](mailto:magarcia@icv.csic.es)

## ABSTRACT

We present a non-invasive method of detecting stress below the elastic limit in magnetic steel elements. The method, based on well-known magnetoelastic effects, relies on mechanical stress-induced permeability modulation. It does not measure absolute values and hence results in suitable *in situ* measurements in situations where small position or vibration changes can change absolute values.

Published under an exclusive license by AIP Publishing. <https://doi.org/10.1063/5.0050402>

## I. INTRODUCTION

Determination of internal stresses in structural materials is crucial to anticipating and preventing failure during service. Therefore, nondestructive testing methods are needed for monitoring of internal stresses in these materials. Iron is present in many structural materials. Of these materials, steel is the most commonly used. In iron-based materials, the ferromagnetic properties of iron can provide a path for external measurement of the stress in an object. Magnetoelastic effects induce coupling between mechanical deformation and the magnetic properties of a material.<sup>1</sup> Hence, any change in the mechanical strain within an object induces a change in its magnetic properties that can be measured to detect mechanical effects. Various methods have been developed for the magnetic measurement of internal stress.<sup>2–5</sup> These methods have been used extensively in practical applications,<sup>6–16</sup> which can be used *in situ* differently from other laboratory techniques as XRD.<sup>17</sup>

According to various reports, magnetoelasticity-based measurement procedures can be classified into two types: (a) direct measurement of the permeability of the object whose internal stress distribution is to be determined and (b) use of sensing elements, such as magnetostrictive amorphous ferromagnets, with the ability

to detect local strains. The sensing element-based method, where the sensor must be clamped at successive positions where the stress is to be measured, can be inconvenient for long samples such as railways.

In a recent paper,<sup>18</sup> we proposed a method of measuring mechanical strain using static magnetic fields. The method involves measuring the magnetostatic field created by an object that has been biased using an external magnet. The main issue that limits the application of this method in facilities is that small displacements or vibrations that change distances can induce measurement error. One path to overcoming this limitation is the use of AC fields and instead of measuring modulus, measure rates or phase differences between quantities that are less affected by small displacements.

In this paper, we analyze the possibility of detecting the maximum mechanical stresses of iron-based materials by measuring the magnetic induction delays in such materials. Thus, we measured permeabilities and delays simultaneously as functions of the applied load. The results confirm the good ability of the phase shift to describe the stress state of the sample. Therefore, we propose a new method that uses AC fields, which may offer important advantages over existing methods with regard to sensitivity, robustness, and simplicity. The method relies on mechanical stress-induced modulation of magnetic permeability.

Although the case analyzed here represents an “a” type measurement, the study of the sensitivity of the delay to the stress is important. If the phase shift of the magnetization with respect to the applied field is a robust index that can be used to detect the internal stress, it should be easier to measure than the permeability and should not require placement of coils around. This provides a substantial advantage when long samples are fixed in position.

II. THEORY

Consider a magnetic cylinder with radius  $R$  and relative permeability  $\mu_r$ . The cylinder has primary and secondary coils [see Fig. 1(b)]. Upon application of AC electrical current to the primary coil, a field  $H_0$ , which is oriented along the cylinder axis or  $z$  axis, appears in the cylinder and the magnetization fluctuates with the frequency of the electrical current. The magnetization fluctuates in phase with the current at low frequencies, but delays appear at high frequencies.

Delays appear at high frequencies because the effective field acting on each surface with radius  $r < R$  is not only the applied field  $H_0$  but also the field created by eddy currents. This latter field

follows Ohm’s law,  $j = \sigma E$ , where the conductivity of a metal is  $\sigma \sim 10^7 \Omega^{-1} m^{-1}$ .

The electric field responsible for the currents is generated by the variation in  $B$  with time  $t$  according to  $\nabla \times E = -\frac{\partial B}{\partial t} = -\mu_0 \mu_r \frac{\partial H}{\partial t}$ . In this equation,  $\mu_0 \mu_r$  is the product of the vacuum and relative magnetic permeabilities of the medium. The  $H$  field created by these currents, which is also oriented along the  $z$  axis, is determined using  $\nabla \times H = j$ . From these two equations, taking curl in both terms of the first one, we obtain

$$\nabla^2 H = \mu_0 \mu_r \sigma \frac{\partial H}{\partial t} \tag{1}$$

If we assume that the sinusoidal profile of  $H$  can be described as  $H(r, t) = H(r)e^{i\omega t}$  and write (1) in cylindrical coordinates, we get

$$\frac{1}{r} \frac{\partial}{\partial r} \left( r \frac{\partial H}{\partial r} \right) = i\sigma \mu_0 \mu_r \omega H \tag{2}$$

This can be rewritten as

$$\frac{d^2 H}{dr^2} + \frac{1}{r} \frac{dH}{dr} - k^2 H = 0, \tag{3}$$

where  $k^2 = i\sigma\mu\omega$ . That is,  $k = (1 + i)\sqrt{\frac{\sigma\mu_0\mu_r\omega}{2}}$  and  $\omega = 2\pi\nu$ . Equation (3) is the modified Bessel equation of order zero, and therefore the solution is

$$H(r) = AI_0(kr) + BK_0(kr). \tag{4}$$

Since  $K_0(kr)$  diverges for  $r = 0$ , where  $H$  is obviously finite, only the term  $A \cdot I_0(kr)$  has physical meaning. The boundary condition  $H(R) = H_0$  leads to the determination of  $A = \frac{H_0}{I_0(kR)}$ . Hence, the field can be written as

$$H = H_0 \frac{I_0(kr)}{I_0(kR)}. \tag{5}$$

The average magnetic induction inside the cylinder is

$$\langle B \rangle = \frac{\mu_0 \mu_r H_0}{I_0(kR) \pi R^2} \int_0^R I_0(kr) 2\pi r dr = \frac{2}{kR} \frac{\mu_0 \mu_r H_0}{I_0(kR)} I_1'(kR), \tag{6}$$

where  $I_1'$  is the first derivative of  $I_0(kR)$ . Since  $B$  fluctuates periodically according to the frequency  $\omega$ , a voltage proportional  $i\omega \langle B \rangle$  is induced in the secondary coil. Hence, the effective permeability  $\mu_{ef} = \langle B \rangle / H_0$  is

$$\mu_{ef} = \mu_0 \mu_r \frac{2I_1'(kR)}{kRI_0(kR)}. \tag{7}$$

If we consider a frequency of 1 kHz, relative permeability of 500, and conductivity of  $10^7 \Omega^{-1} m^{-1}$ , which are typical

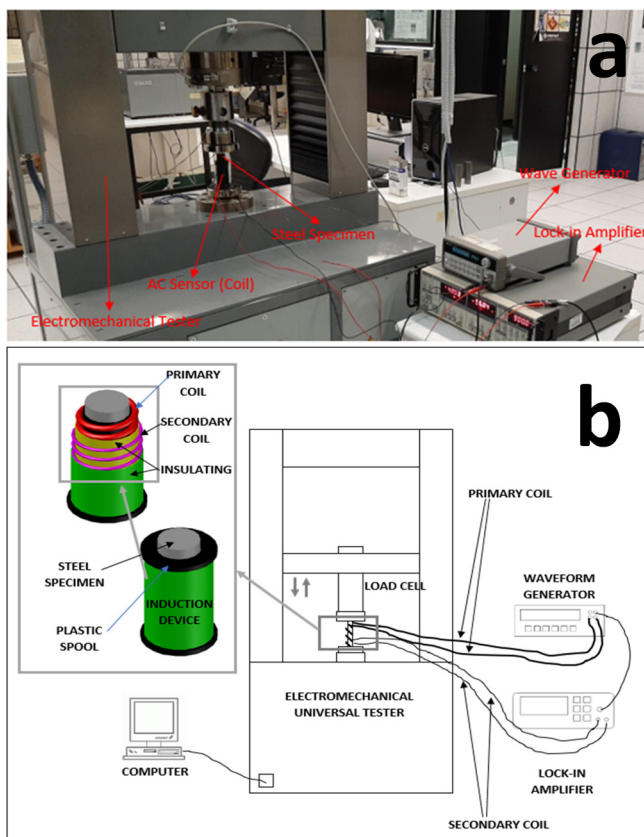


FIG. 1. (a) Image and (b) sketch of the experimental setup.

for steel, we get

$$k = (1 + i) \sqrt{\frac{\sigma \mu_0 \mu_r \omega}{2}} = 4 \cdot 10^3 (1 + i) \text{ (m}^{-1}\text{)}. \quad (8)$$

At 1 MHz, we obtain

$$k = (1 + i) \sqrt{\frac{\sigma \mu_0 \mu_r \omega}{2}} = 1.2 \cdot 10^5 (1 + i) \text{ (m}^{-1}\text{)}. \quad (9)$$

If we consider a permeability of 100 (instead of 500), the  $k$  value is approximately halved. At a conductivity of  $10^6 \Omega^{-1} \text{ m}^{-1}$ , the modulus of  $k$  is divided by three. In any case, we can assume that we will consider  $k$  values between  $10^3$  and  $10^6 \text{ m}^{-1}$ .

At  $kR \gg 1$ , which is satisfied for steel cylinders with radii larger than 1 cm, we can perform an approximation using

$$\frac{\mu_{\text{ef}}}{\mu_0 \mu_r} = \frac{\sqrt{2}}{|kR|} \left( 1 + \frac{1}{8(kR)^2} + \dots \right). \quad (10)$$

The delay  $\epsilon$  in the average induction,  $\langle B \rangle e^{i(\omega t + \epsilon)}$ , with respect to  $H_0$  (that is, of  $\mu_{\text{ef}}$  with respect to  $\mu_0 \mu_r$ ) must be so. Thus, the first term in (10) is real. Therefore,  $\frac{\text{Im} \mu_{\text{ef}}}{\text{Re} \mu_{\text{ef}}} = \frac{\sqrt{2}}{|kR|} = \tan \varphi = \frac{1}{\tan \epsilon}$ . According to (8), the first order approximation of this equation is

$$\tan \epsilon = \frac{|kR|}{\sqrt{2}}. \quad (11)$$

Next, we address the dependence of dephasing on the applied mechanical stress. According to Ref. 9, if the frequency of  $H_0$  is constant, the delay can vary only if the magnetic permeability varies. For macroscopic polycrystalline materials, the permeability can vary because texturing induces grain orientation or residual stress coupling via magnetoelastic effects. These effects are not independent since texturing induces stress fields.

We can then use (11) to estimate the sensitivity of the delay to the change in the applied stress,  $\tau$ ,

$$\frac{\partial \tan \epsilon}{\partial \tau} = \frac{\partial R \sqrt{\sigma \omega \mu}}{\partial \mu} \frac{\partial \mu}{\partial k^*} \frac{\partial k^*}{\partial \tau}, \quad (12)$$

where  $k^*$  represents the anisotropy constant.

According to Ref. 12, the phase angle varies with the change in the anisotropy constant and, therefore, as indicated by (12), with the applied stress. Since we know how the anisotropy constant varies with the applied stress (i.e.,  $\frac{\partial k^*}{\partial \sigma}$ ), the dependence of the permeability on the mechanical stress can be determined by knowing the derivative  $\frac{\partial \mu}{\partial k^*}$ . However, this derivative is known only when the dependence of permeability on the anisotropy constant is known. Typically, this dependence is affected by several different variables and is difficult to predict. First, it depends on the magnetic structure of the material, which is characterized by the grain size, crystalline symmetry, and the presence of texture. However, it also depends on the magnetization process, which can occur via domain wall motion, magnetization rotation, or a combination of both. Consequently, the function that links the permeability to the

anisotropy also depends on the domain structure, which depends on the previous history of the material. Finally, the sensitivity of the magnetic permeability to the stress is determined primarily by the magnetostriction-to-anisotropy ratio. This ratio is the figure of merit that characterizes the quality of any magnetoelastic stress sensor. Therefore, one can easily determine  $\frac{\partial \mu}{\partial k^*}$  by performing a direct measurement of the permeability as a function of the applied stress using a sample of the material to be tested. It is interesting to note that the magnetization process can be affected by changes in the applied field frequency and strength. Thus, laboratory tests must be performed using the applied field frequency and strength that will be used during the final measurement process.

We can consider a polycrystalline steel beam. The beam is not textured but has cubic crystalline symmetry, saturation magnetization of the order of 1 T, an anisotropy constant in the absence of stress  $k_m^*(0)$  of  $\sim 5 \times 10^4 \text{ J m}^{-3}$ , and a magnetostriction constant of  $\sim 7 \times 10^{-6}$ .<sup>11</sup> It is well known that the introduction of stress into a magnetoelastic material modifies its anisotropy constant,  $k_m(\sigma)$  by an amount that, according to the first order Taylor expansion, can be written as

$$k_m(\sigma) = k_m^*(0) + \left( \frac{\partial k_m^*}{\partial \sigma_{ij}} \right)_0 \sigma_{ij}, \quad (13)$$

where  $\left( \frac{\partial k_m^*}{\partial \sigma_{ij}} \right) = \lambda_{m,ij}$  is the magnetostriction constant of the material. The exact dependence of the magnetic permeability on the mechanical stress is difficult to determine. However, we can estimate the change in magnetic anisotropy induced by the stress, as this quantity must be on the order of  $\sim \lambda_{m,ij} \sigma_{ij}$ . Thus, an anisotropy change of  $2 \times 10^3 \text{ J m}^{-3}$  can be achieved by applying a stress of  $\sim 200 \text{ MPa}$ . This represents a variation in anisotropy of the order of 5%. Such an anisotropy variation is expected to induce permeability changes of the same order of magnitude, and these changes are expected to be detectable.

It is also well established<sup>19</sup> that the magnetoelastic anisotropy  $E_{me}$  of a polycrystalline material can be expressed as a function of the angle  $\theta$  between the spontaneous magnetization and the applied stress,  $\tau$ ,

$$E_{me} = -\frac{3}{2} \lambda_s \tau \cdot \cos^2 \left( \theta - \frac{1}{3} \right), \quad (14)$$

where  $\lambda_s$  is the average magnetostriction coefficient. For a cubic crystal, this can be approximated using  $\lambda_s = \frac{2\lambda_{100} + 3\lambda_{111}}{5}$ . The easy axis becomes parallel or perpendicular to the longitudinal beam direction according to the sign of the product  $\lambda_s \tau$ .

In one section of the beam, the stresses applied by the rest of the beam through its transverse sections generate uniaxial anisotropy that should be superimposed onto the existing magnetocrystalline anisotropy. The magnetoelastic anisotropy energy provides an illustrative example of the complex relation between permeability and anisotropy. According to (14), the application of an external stress is equivalent to introducing uniaxial anisotropy. New uniaxial anisotropy can promote  $90^\circ$  domain wall displacement as well as magnetization rotation (no pressure is exerted on  $180^\circ$  domain walls). This domain wall motion is generally irreversible. Therefore,

the domain structure present after removing the stress is expected to be different from the one that was present before application of external stress. Consequently, the magnetic permeability measured before applying the stress should be different from that obtained after removing it. Magnetoelastic hysteresis reflects only the hysteresis caused by 90° domain wall motion. By measuring the magnetoelastic hysteresis of torsion, Hernando *et al.*<sup>20</sup> showed that this hysteresis can be removed by applying a demagnetizing field prior to each permeability measurement.

To illustrate the influence of this uniaxial anisotropy on the magnetic permeability in a qualitative manner, we assume that the magnetization process is governed mainly by domain wall motion. The magnetic susceptibility increases if the easy axis for magnetoelastic anisotropy coincides with the field direction, but it decreases if the easy axis becomes perpendicular to the field direction. The opposite trend would be observed if the magnetization process were driven by pure magnetization rotation.

Finally, we can estimate the expected susceptibility variation for a case where the magnetization process corresponds to pure rotation and the magnetoelastic easy axis is perpendicular to the applied field. In this case, the relative permeability  $\mu_r$  can be expressed as a simple function of  $k^*$ ,

$$\mu_r = \frac{M_s^2}{k^*}. \tag{15}$$

Then,

$$\frac{\partial \tan \epsilon}{\partial k^*} = \frac{\partial R \sqrt{\tau \mu_0 \mu_r \omega}}{\mu_0 \partial \mu_r} \mu_0 \partial \mu_r = -\frac{R}{2\sqrt{\sigma \mu_0 \mu_r \omega}} \frac{\mu_0 M_s^2}{k^{*2}}, \tag{16}$$

where we assume that  $\mu_r = \frac{M_s^2}{k^*}$ , where  $M_s$  represents the spontaneous magnetization of the cylinder and  $\mu = \mu_0 \mu_r$ . This dependence is strictly valid for pure magnetization rotation in uniaxial magnetocrystalline grains. However, this simple expression is used here as a simplified method of estimating the phase shift produced by internal stress fluctuations. The internal stress distribution is a source of local variation in  $k^*$  in macroscopic samples. It yields an average local anisotropy perturbation of  $(3/2)\lambda_s \tau$ , where  $\lambda_s$  and  $\tau$  are the magnetostriction constant and the local stress averaged over the measuring volume, respectively. After determining the value of  $\Delta k^*$ , (12) becomes

$$\Delta \tan \epsilon = \frac{3R}{4\sqrt{\sigma \mu_0 \mu_r \omega}} \frac{\mu_0 M_s^2}{k^{*2}} \lambda_s \tau. \tag{17}$$

Thus, the relative variation in the delay is

$$\frac{\Delta \tan \epsilon}{\tan \epsilon} = \frac{3\mu_0 M_s^2}{4\sigma \mu_0 \mu_r \omega k^{*2}} \lambda_s \tau. \tag{18}$$

Typical values for a cylindrical sample include  $M_s = 10^8 \text{ Am}^{-1}$ ,  $k^* \approx 10^4$  or  $10^5 \text{ J m}^{-3}$ ,  $\lambda_s = 10^{-6}$ , conductivity  $\sigma \sim 10^6 \text{ } \Omega \text{ m}$ ,

$\mu_r \sim 10^2$ , and  $\omega \sim 10^4 \text{ Hz}$ . This produces

$$\frac{\Delta \tan \epsilon}{\tan \epsilon} = \frac{3M_s^2}{4\sigma \mu_r \omega k^{*2}} \lambda_s \tau = \frac{4 \cdot 10^2}{\sigma \mu_r \omega} \tau \approx 4 \cdot 10^{-10} \tau (\text{MPa}). \tag{19}$$

Thus, mechanical stress of the order of 200 MPa (about half of the elastic limit of steel) induces relative variation of the delay between the applied field and the induced current on the order of 8%. This provides a method of detecting internal stress well before failure.

In order to apply the method suggested in this report, a careful magnetic and magnetoelastic study of the material must be performed to determine the relationship between the permeability and the anisotropy constant  $k^*$  accurately. Equations (15)–(19) hold only for the particular case of pure magnetization rotation when the easy axis is perpendicular to the applied field, i.e., to the longitudinal beam direction. Even though this condition is not fulfilled in the real environment, it provides an estimate of the sensitivity of the permeability to the applied stress.

### III. EXPERIMENTAL METHOD

We designed and fabricated an experimental apparatus in order to verify these results experimentally. Figure 1(a) shows a picture of the homemade magneto-mechanic device, whereas Fig. 1(b) presents a scheme of the system. The system included an induction device consisting of a primary coil with 200 turns with a wire diameter of 0.5 mm and a secondary coil of 100 turns with a wire diameter of 0.17 mm over a plastic spool. The coil had an internal radius of 27 mm and a length of 80 mm.

Two specimens were tested. They corresponded to cylinders that were 100 mm length and had radii of 23 mm. One specimen was made of SR235JR steel, whereas the other was made of F-114 steel. SR235JR includes 0.17% C and 1.4% Mn, whereas F-114 contains 0.45% C and 0.65% Mn. The latter alloy provides superior mechanical properties.

For the experiments, the samples were placed inside the induction device and the primary coil was connected to a Hewlett Packard 33120A wave generator to obtain a 4 V (PP) amplitude sine wave at a frequency of 40 kHz. The secondary coil was connected to the input of a SRS844 lock-in amplifier from Stanford Research Systems. The output of the wave generator was used as reference signal in the lock-in amplifier. The specimens were placed in an electromechanical universal tester EM2/200/FR from Microtest to apply controlled compressive stress.

### IV. RESULTS

The phase ( $\epsilon$ ) variation in the secondary coil signal was measured using a 0–200–0 MPa charge–discharge cycle during which a 4 V (PP) signal at 40 kHz was applied to the primary coil.

Figure 2 shows dephasing during load cycles at 40 kHz for both samples. The curves are quite similar and indicate an increase in dephasing of  $\sim 3.9\%$  for a 100 MPa load. In addition, both curves exhibit the typical magnetoelastic hysteresis referenced above, which has a magnetic, but not mechanical, origin since we are well below the elastic limits of the steel samples. Even though the stress is always within the elastic range, it induces irreversible magnetic

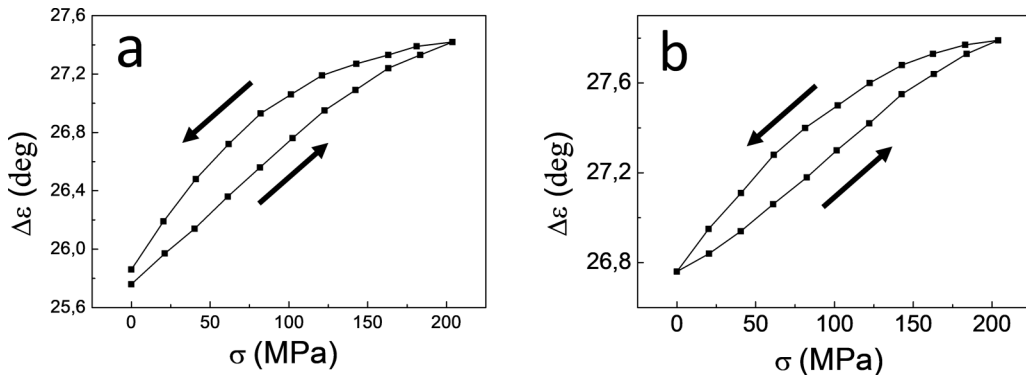


FIG. 2. The change in dephasing as a function of the applied load for (a) SR235JR and (b) F-114 steel specimens at 40 kHz. The arrows indicate the loading and unloading branches.

rearrangements ( $90^\circ$  domain wall motion). It is known that such hysteresis can be eliminated by demagnetizing the sample before measuring the phase at each applied stress. Demagnetization requires the application of an AC magnetic field with a decreasing amplitude. The maximum demagnetizing field applied should be strong enough to produce technical saturation of the sample. This

rather tedious procedure should allow us to obtain a single permeability for any residual stress, independent of the history of the material. However, phase detection is enough for a quick estimation of the maximum internal stress. The laboratory-based material test plotted in Fig. 3 should be performed using an applied field whose intensity and frequency are the same as those used in the

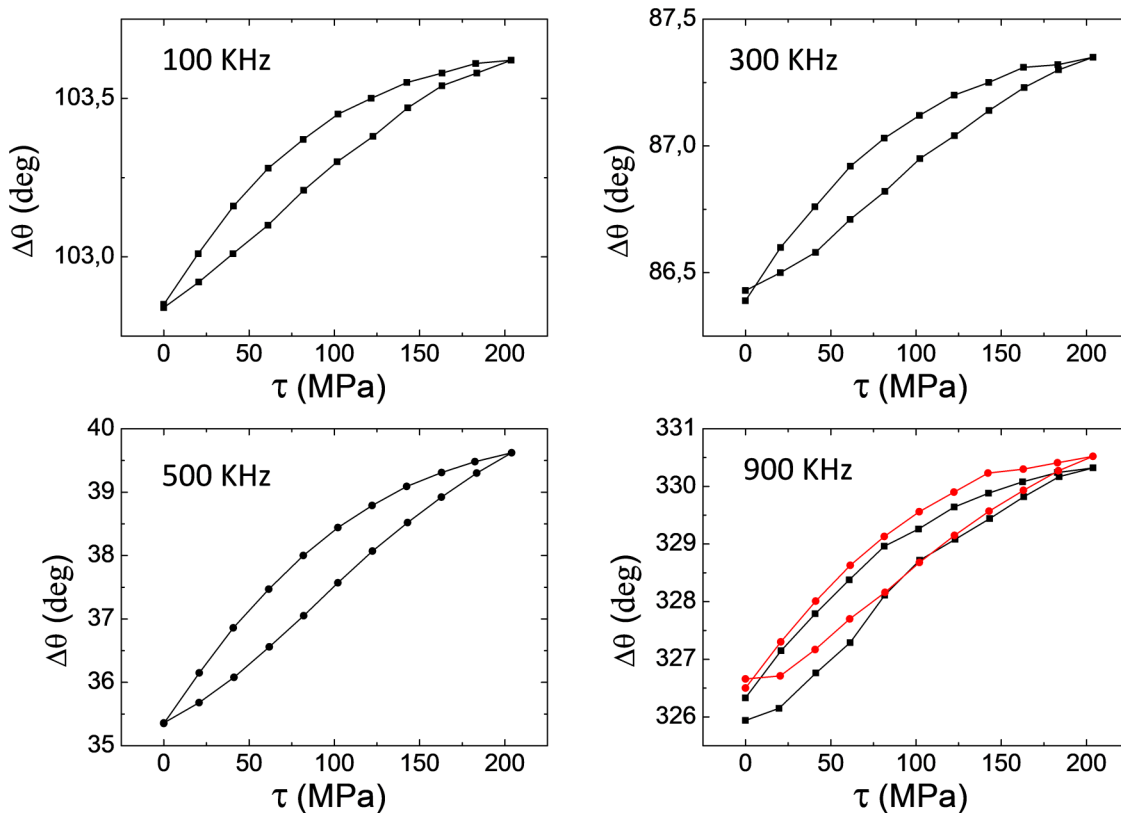


FIG. 3. Measurement of the SR235JR sample at various frequencies. The experiment performed at 900 kHz was repeated to confirm reproducibility.

subsequent *in situ* testing procedure. One can obtain the average  $\Delta\epsilon$  for any stress  $\tau$  using the results of Fig. 2. One can also determine the hysteresis for the particular field characteristics that have been applied. If the safety condition indicates that 200 MPa is the upper allowed limit for  $\tau$ ,  $\Delta\epsilon$  should be smaller than 27.7 if hysteresis is disregarded. According to the curves in Fig. 2, for a given  $\tau$ , there is a maximum  $\Delta\epsilon$  uncertainty of  $\pm 0.4$  as a consequence of magnetoelastic hysteresis. Therefore, the *in situ* maximum measured  $\Delta\epsilon$  should be lower than 27.5 to ensure that the maximum stress remains below 200 MPa. Thus, these measurements indicate that the phase is a good parameter to use for quick detection of stress fluctuation upper limits and that the theoretically predicted dependence is in good accordance with the experimental results.

According to (16), dephasing should change by  $\sim 1\%$  for type “a” measurements at  $\omega \sim 4 \cdot 10^4$  Hz. That this is the order of magnitude that is observed experimentally (3.9%) confirms the reliability of the method.

We performed measurements at several frequencies in order to confirm the reliability and reproducibility of the method. Figure 3 shows results for the SR235JR material at various frequencies. The experiment was repeated at 900 kHz. Differences between equivalent experiments are less than 10% of the variation induced by the applied stress.

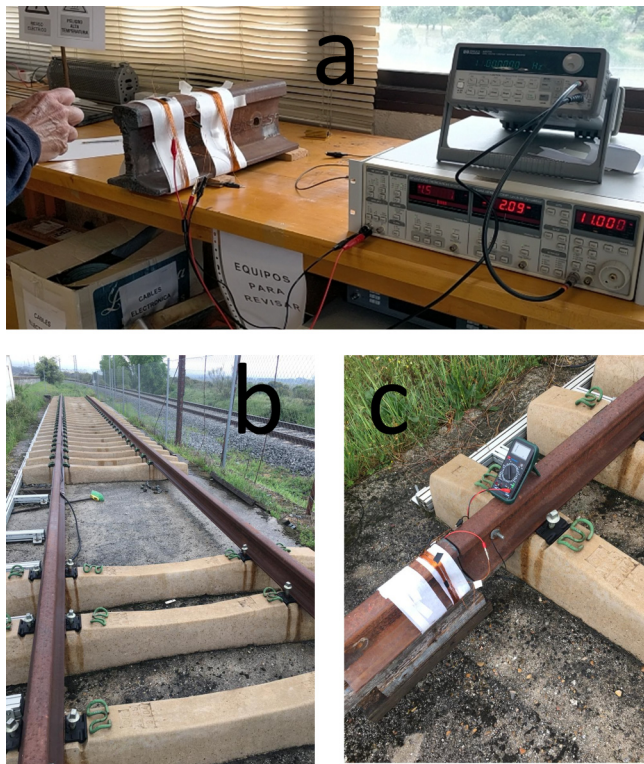


FIG. 4. Pictures showing the (a) experimental railway apparatus used in the lab, (b) test railway used for experiments performed outside, and (c) detail of the apparatus used in the experiments. Multimedia view: <https://doi.org/10.1063/5.0050402.1>

## V. TESTS PERFORMED IN A RAILWAY ENVIRONMENT

In order to perform measurements under conditions that are similar to those in the field, we performed measurements by placing primary and secondary coils with 30 turns over a piece of railway that was 80 cm in length, as shown in Fig. 4(a) (Multimedia view). This railway section had a rail head of 7 cm, a rail base of 15 cm, and 1.3 cm rail web.

Since laboratory environment temperature variations are small enough to generate large stresses via thermal expansion,<sup>21,22</sup> we induced permeability changes in the rail by applying DC magnetic fields. The change in permeability induced by the applied stress,  $\tau$ , can be compared quantitatively with that produced by the DC field,  $H$ , by estimating the energy density, which depends on the magnetization orientation with respect to the directions in which the DC field and stress are applied. The magnetoelastic energy density is given by (14). Accordingly, the maximum torque exerted by the stress on magnetization toward the easy axis is on the order of  $\lambda_s \tau$ . In the case of an applied field, the maximum torque is of the order of  $\mu_0 M_s H$ . By considering approximate values of  $\lambda_s = 10^{-6}$  and  $\mu_0 M_s = 1$  T, one can infer that the maximum torque applied to magnetization upon applying a field of  $100 \text{ A m}^{-1}$  is equivalent to the maximum torque exerted by an applied stress of 100 MPa, i.e., the effects of  $1 \text{ A m}^{-1}$  and 1 MPa are equivalent.

Thus, an applied field is produced by approaching the rail with a magnet. This NdFeB magnet is cylindrical, 3 cm in diameter, and 0.5 cm tall. It generates a non-uniform magnetic field in the measurement volume. A maximum average value of a few Gauss is reached at the closer position of the magnet with respect to the rail (6.5 cm). It is interesting to note that the effect of the non-uniformity that the applied field induced on the magnetic permeability is similar to that produced by the non-uniform stresses developed in the measurement volume. In fact, the rail normally experiences residual stresses, including tension stress at the base and head of the rail and compressive stress at the rail web. These stresses are on the order of 200 MPa.

The video in the Multimedia View shows how, upon placing a permanent magnet 6.5 cm from the measurement volume, we observe phase variations of  $\sim 50\%$  at a frequency of 40 Hz.

We subsequently repeated the experiment on a railway. The test is shown in Fig. 4(b) and includes the placement of two coils [Fig. 4(c)]. Using a frequency of 1 kHz, we obtain a phase variation of 1.6% when placing the magnet at a distance of  $\sim 8$  cm. At a lower frequency of 40 Hz, variation of up to 17% is observed.

It is interesting to note that the non-uniformity of the applied field should induce a magnetic permeability effect similar to that produced by non-uniform stresses in the measuring volume.<sup>22</sup> The rail normally undergoes residual stresses, including tension stress at the base and head of the rail and compressive stress at the rail web. These stresses are on the order of 200 MPa. Thus, regardless of the method used, stress detection determines the average stress across the measuring volume, which in this case is the rail volume covered by the secondary coil. The permeability fluctuations generated by the action of the non-uniform field and reflected in the measured phase shift indicate that this method should be capable of detecting non-uniform stresses.

## VI. CONCLUSIONS

In summary, we demonstrated that measuring changes in the phase difference between the magnetization and the applied field provides an interesting approach to the problem of residual stress fluctuation measurement. A large number of laboratory experiments were performed. The results indicated that the measurement procedure is reliable and robust. Since the method relies on phase measurements, it is not affected by small changes in positions or vibrations. Thus, it is suitable for *in situ* sensors. In typical structural steels, the changes are of the order of a few percent at half of the elastic limit. As confirmed by experiments carried out on railway tracks, it should be possible to measure residual stress fluctuations along the lengths of steel elements while they are in service.

## ACKNOWLEDGMENTS

We thank Daniel García, Alberto González, and Victor Zamoro for technical support. This work was supported by the Spanish Ministerio de Ciencia, Innovación y Universidades through Research Project No. MAT2017-86450-C4-1-R, by the Comunidad de Madrid through Project Nos. S2013/MIT-2850 (NANOFROTMAG) and P2018/NMT-4321, and by a research Ph.D. grant from the Research Vice-Rectorship of Nebrija University.

## DATA AVAILABILITY

The data that support the findings of this study are available from the corresponding author upon reasonable request.

## REFERENCES

- <sup>1</sup>A. del Moral, *Magnetostriction: Basic Principles and Materials* (IOP Publishing, 2003).
- <sup>2</sup>D. C. Jiles, "Review of magnetic methods for nondestructive evaluation," *NDT Int.* **21**(5), 311–319 (1988).
- <sup>3</sup>M. K. Devine, D. C. Jiles, A. R. Eichmann, D. A. Kaminski, and S. Hardwick, "Magnescope: Applications in nondestructive evaluation," *J. Appl. Phys.* **73**(10), 5617–5619 (1993).
- <sup>4</sup>P. Vourna, A. Ktena, P. E. Tsakiridis, and E. Hristoforou, "An accurate evaluation of the residual stress of welded electrical steels with magnetic Barkhausen noise," *Measurement* **71**, 31 (2015).
- <sup>5</sup>H. Kwun, "A nondestructive measurement of residual bulk stresses in welded steel specimens by use of magnetically induced velocity changes for ultrasonic waves," *Mater. Eval.* **44**(13), 1560–1566 (1986).
- <sup>6</sup>A. P. S. Baghel, B. Sai Ram, L. Daniel, S. V. Kulkarni, G. Krebs, J. B. Blumenfeld, and Santandrea, "An alternative approach to model mechanical stress effects on magnetic hysteresis in electrical steels using complex permeability," *Comput. Mater. Sci.* **166**, 96–104 (2019).
- <sup>7</sup>J. M. Makar and B. K. Tanner, "The *in situ* measurement of the effect of plastic deformation on the magnetic properties of steel: Part II—Permeability curves," *J. Magn. Magn. Mater.* **187**, 353–365 (1998).
- <sup>8</sup>G. Dobmann, I. Altpeter, B. Wolter, and R. Kern, "Industrial applications of 3MA-micromagnetic multiparameter microstructure and stress analysis," *Stud. Appl. Electromagn. Mech.* **31**, 18 (2008).
- <sup>9</sup>D. Miyagi *et al.*, "Influence of compressive stress on magnetic properties of laminated electrical steel sheets," *IEEE Trans. Magn.* **46**(2), 318–321 (2010).
- <sup>10</sup>M. G. Maylin and P. T. Squire, "The effects of stress on induction, differential permeability and Barkhausen count in a ferromagnet," *IEEE Trans. Magn.* **29**(6), 3499–3501 (1993).
- <sup>11</sup>R. M. Bozorth, "Stress and magnetization" in *Ferromagnetism* (Van Nostrand, New York, 1951).
- <sup>12</sup>M. Oka and M. Enokizono, "Evaluation of a reverse-side defect on stainless steel plates by the residual magnetic field method," *IEEE Trans. Magn.* **37**(4), 3073–3076 (2001).
- <sup>13</sup>T. Uchiyama, P. Sompob, K. Mohri, and N. Ishikawa, "Nondestructive evaluation for structuring steel deformation using amorphous wire MI sensor," *J. Magn. Soc. Jpn.* **23**(4–2), 1465–1468 (1999).
- <sup>14</sup>J. M. Barandiaran, G. V. Kurlyandskaya, D. de Cos *et al.*, "Multilayer magnetoimpedance sensor for nondestructive testing," *Sens. Lett.* **7**, 374–377 (2009).
- <sup>15</sup>F. Vacher and F. G. P. Alves, "Eddy current non-destructive testing with giant magnetoimpedance sensor," *NDT&E Int.* **40**, 439–442 (2007).
- <sup>16</sup>R. Szewczyk, "Generalization of the model of magnetoelastic effect: 3D mechanical stress dependence of magnetic permeability tensor in soft magnetic materials," *Materials* **13**(18), 4070 (2020).
- <sup>17</sup>X. Huang, Z. Liu, and H. Xieba, "Recent progress in residual stress measurement techniques," *Acta Mech. Solida Sin.* **26**(6), 570–583 (2013).
- <sup>18</sup>M. S. García Alonso, F. Giacomone, A. Pérez, I. Kaiser, J. F. Fernández, A. Hernando, J. Vinolas, and M. A. García, "Magnetoelastic determination of variations of internal stress in magnetic steels," *AIP Adv.* **10**, 115302 (2020).
- <sup>19</sup>S. Chikazumi and C. D. Graham, *Physics of Magnetism* (Oxford Science, 2009).
- <sup>20</sup>A. Hernando, V. Madurga, and M. Vazquez, "Hysteresis magnetoelástica de torsión," *An. Fis.* **72**, 253–257 (1976).
- <sup>21</sup>E. Johnson, "Measurement of forces and neutral temperatures in railway rails—An introductory study," Building Technology and Mechanics, Report no. 2004 11, Boras, Sweden, 2004.
- <sup>22</sup>P. T. Zwierczyk and K. Varadi, "Thermal stress analysis of a railway wheel in sliding-rolling motion," *J. Tribol.* **136**, 031401 (2014).